Mechanics and Mechanical Engineering
Vol. 10, No 1 (2006) 8–20
© Technical University of Lodz

Friction Induced Vibration in Conveying Belt-Roller System

Kazimierz Furmanik
AGH University of Science and Technology
30-059 Kraków, al. Mickiewicza 30, Poland
fukaz@agh.edu.pl

Andrzej Stefański and Jerzy Wojewoda
Technical University of Łódź, Division of Dynamics
Stefanowskiego 1/15, 90-924 Łódź, Poland

Received (9 May 2006)
Revised (20 May 2006)
Accepted (3 June 2006)

In the paper analysis of the roller vibration in the conveyor belt-roller friction support system is presented. Influence of some system parameters to the vibration level and possibilities of control and limitation of vibration are shown.

Keywords: Rolling pair, friction induced vibration, fatigue life, conveyor belt.

1. Introduction

Increasing demand of usability and durability of machines and tools is directly connected to necessity of improving of design in aspects of safety, strength, silent work, durability etc. One of many reasons when such problems fail in practice can be friction induced vibrations [1, 5, 6, 7, 8]. In conveying belt systems the vibration can occur in numerous places where the belt contacts with rollers, which support and guide it along the path. Such vibration cause friction wear of the belt material and covers of the rollers, and also fatigue cracks of mounting elements along the track. They also are the main source of noise. Centering rollers are used for proper positioning of the belt and improving guidance. Appropriate choosing of angles of their location and distances between them is essential to proper work of the whole system, its energy consumption, durability of the belt and roller covers. The angle, marked as a is understood as the angle between its axis to the perpendicular position of the belt axis, see Figure 1a.

The angle causes belt slip over rollers cover and friction force which perpendicular projection to the axis belt allows for the belt centering along the path. Vibration

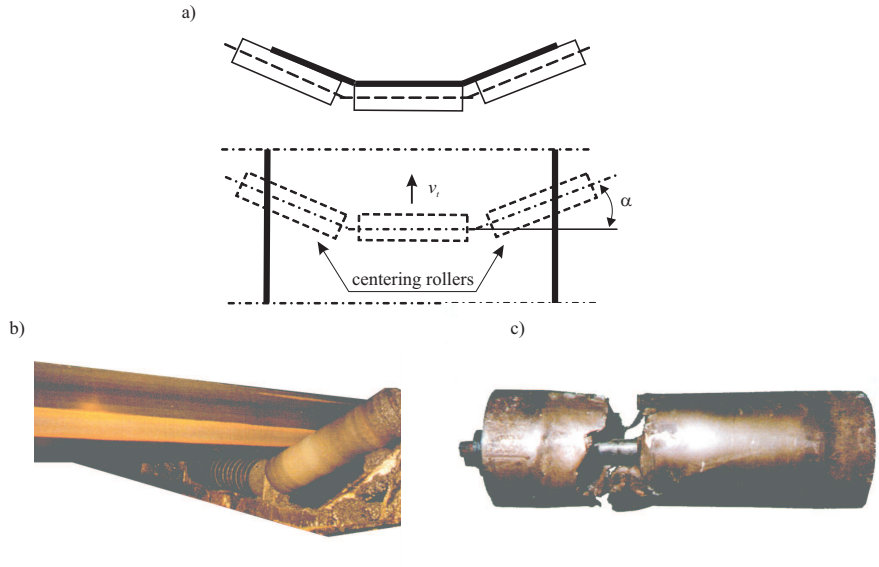

Figure 1 Results of excessive wear during belt slip over the centering roller: a) belt position on the rollers, b) friction wear of the lower cover of the belt (brighter strip), c) abrasion hole of the roller cove

of rollers caused by this force are of different types and quantities characterizing depends on friction characteristics and other parameters of the system. In this paper, using numerical simulations the analysis of the vibration rollers-belt is described and some possibilities of diminishing their level presented.

2. Equations of motion

The analysis of the roller element is based on phenomenological dependence friction on slip velocity on the belt, see Figure 3. Friction characteristics is obtained experimentally with parameters of the belt-roller contact fixed. The following simplifications are assumed:

- vibration of the roller are treated as a whole body are discussed in macro scale,
- analysis of the roller motion is limited to the movement along it axis,
- the support of the roller is modeled as an elasto-viscous Kelvin-Voigt element,
- the geometry of the roller is assumed ideal, its contact with the belt linear and no clearances along the radius occurs,
- temperature and wear effects are not included having no influence to the friction characteristics.

The system shown in Figure 2 is used in analysis of roller vibration along its axis. The belt moving with velocity v_t (Figure 1a) slips with friction with velocity v_p over stiff cover of the roller with mass M along its axis. The roller is connected to the base with elasto-viscous element characterized by constant valued parameters – stiffness K and damping D. Behavior of such system is described with the following equation:

$$M\ddot{X} + D\dot{X} + KX = F\,, \tag{1}$$

where X is displacement of the roller along its axis, $\dot{X} = dX/dt$ is the velocity, t – time, f is the friction coefficient, $F = f\,N\,\mathrm{sign}(v_p)$ the friction force, v_t – the belt velocity, and, $v_p = v_t \sin\alpha - \dot{X}$ is the belt slip velocity over the roller.

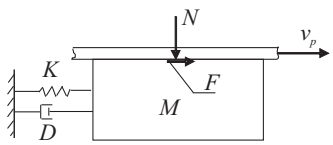

Figure 2 Scheme of the analyzed system

Experimentally obtained friction characteristics is directly related to the roller-belt behavior and described according to the [2,4] as seen in Figure 3:

$$\begin{aligned}
f(v_p) &= 9.5412764|v_p| - 92.876572v_p^2 \quad \text{for } |v_p| \le v_p^* = 0.052m/s\,,\\
f(v_p) &= 0.256198 - 0.2153213|v_p| \text{ for } v_p^{**} > |v_p| > v_p^*\,, \quad v_p^{**} = 0,958 \text{ m/s}\\
f(v_p) &= 0.05 \quad \text{for } |v_p| > v_p^{**}
\end{aligned}$$

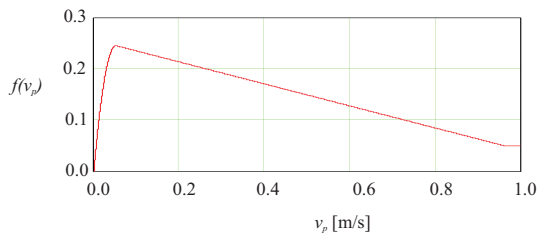

Figure 3 Friction characteristic used

The following system data were used in numerical simulations:

- roller: $\phi 159/\phi 30 \times 465$ with mass $M = 12.2$ [kg];
- elastic coefficient in roller contact: $K = (0.5 \div 2.0) \cdot 10^6$ [N/m];
- viscous coefficient in roller contact: $D = 0 \div 120$ [Ns/m];

- normal force acting on the roller: $N = 10 \div 1000$ [N];
- inclination angle of the roller $\alpha = 0.9 \div 5.0[°]$;
- belt velocity: $v_t = 3.0$ [m/s].

Simulation was performed with use of the software suite PROFESSIONAL VISSIM & ANALYZE ver. 2.0 [9]. Main task of investigation was influence of parameters to the vibration level of the roller.

3. Simulation results

The complete schedule of investigation covered first of all, estimation of the influence of the following to the roller vibration characteristics:

- angle of roller position α (with other parameters fixed),
- elastic coefficient K,
- damping coefficient D,
- force of belt pressure to the roller N.

Figure 4 presents scheme of the simulation program.

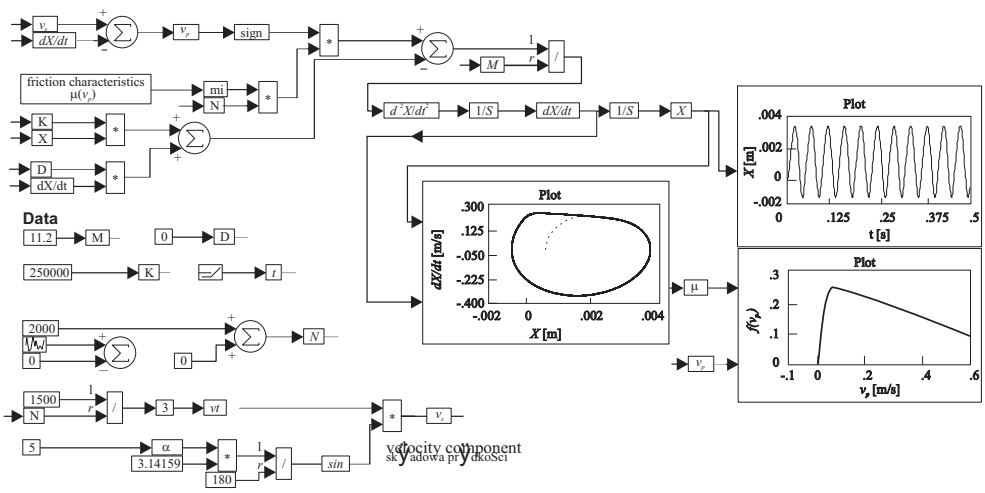

Figure 4 Simulation program flow (VisSim)

Simulation results for: $K = 0.25 \cdot 10^6$ [N/m]; $v_t = 3.0$ [m/s]; $D = 0$ [Ns/m]; $N = 500$ [N] are show in Figures 5 – 7.

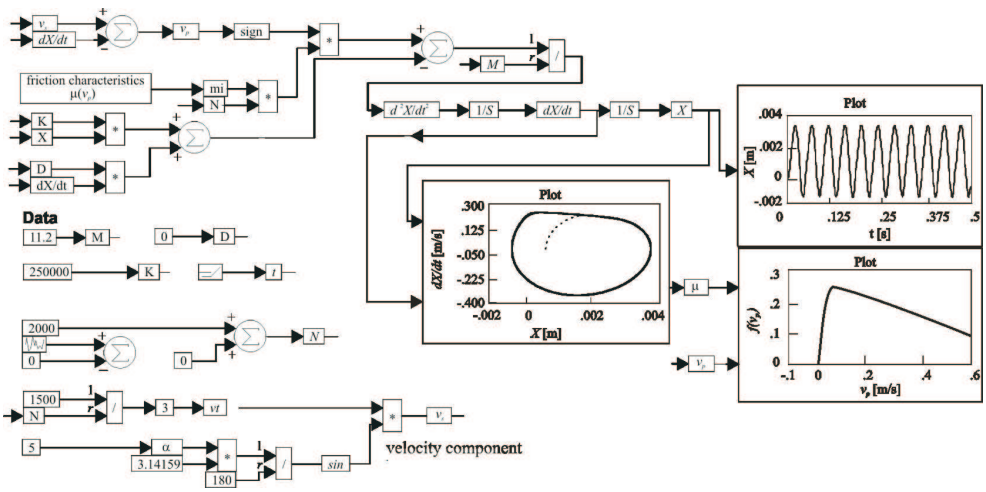

Figure 5 Vibration character at $\alpha = 0.9°$: a) displacement vs. time, b) phase plane, c) friction characteristics

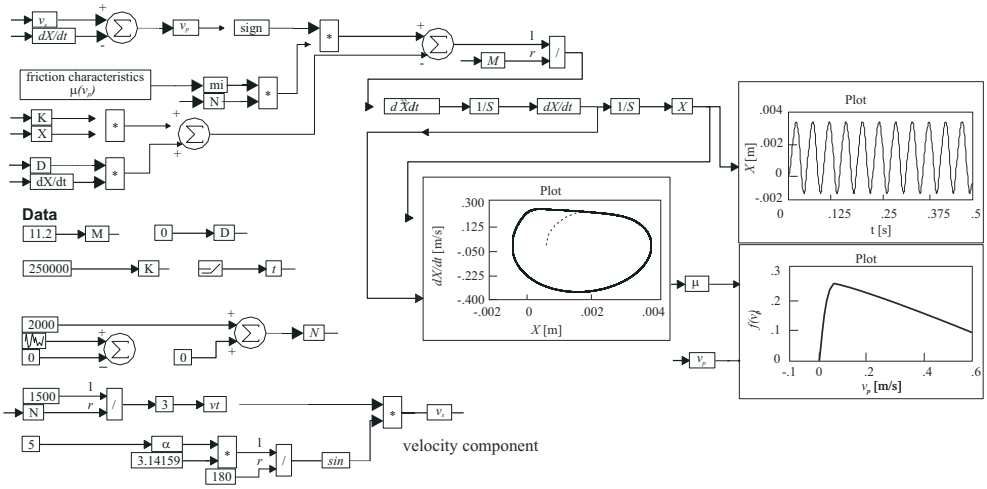

Figure 6 Vibration character at $\alpha = 3.0°$: a) displacement vs. time, b) phase plane, c) friction characteristics

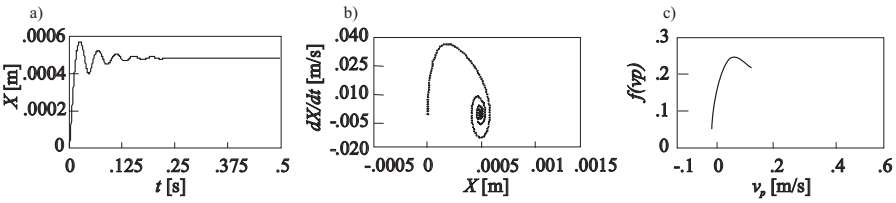

Figure 7 Vibration character at $\alpha = 5.0°$: a) displacement vs. time, b) phase plane, c) friction characteristics

From Figure 5 one can observe for $\alpha \leq 0.9°$ vibration in the system are not induced, and with further increase of the angle the vibration appears and their amplitude increases with frequency almost the same, about 23.7 Hz. Also range of possible work on the friction characteristics increases, see Figures 5c, 6c, 7c.

Then results for parameter values: $v_t = 3.0$ [m/s], $D = 0$ [Ns/m], $\alpha = 3°$, $N = 500$ [N] are shown in Figures 8 and 9.

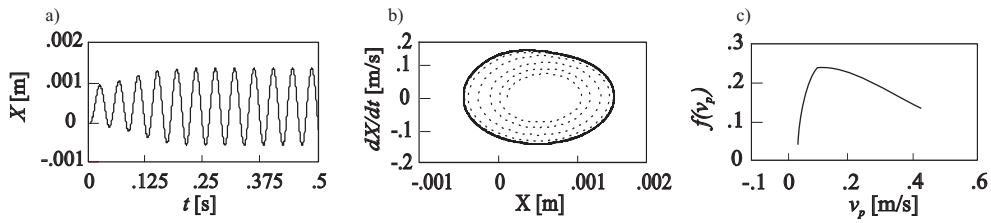

Figure 8 Vibration character at $K = 1.0 \cdot 10^6$ [N/m]: a) displacement vs. time, b) phase plane, c) friction characteristics

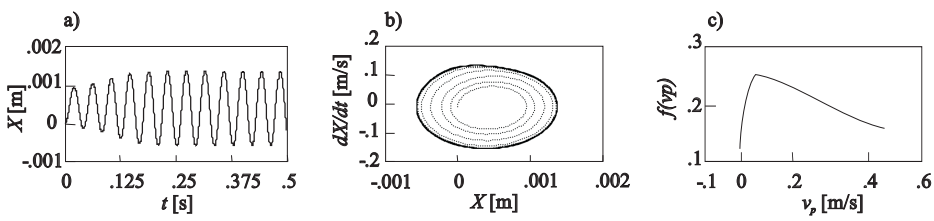

Figure 9 Vibration character at $K = 2.0 \cdot 10^6$ [N/m]: a) displacement vs. time, b) phase plane, c) friction characteristics

Figures 6a, 8a and 9a present behavior, when with increase of the elasticity coefficient the amplitude of the induced vibration diminishes and frequency increases, from 23,7 Hz to 68,1 Hz, while range of work stays similar on the friction characteristics.

Further simulations changes of damping are taken into account with other parameters fixed at: $v_t = 3{,}0$ [m/s]; $K = 0{,}5{\cdot}10^6$ [N/m]; $N = 500$ [N], $\alpha = 3$ [$^\circ$]. The results are presented in Figures 10 $\div$ 13.

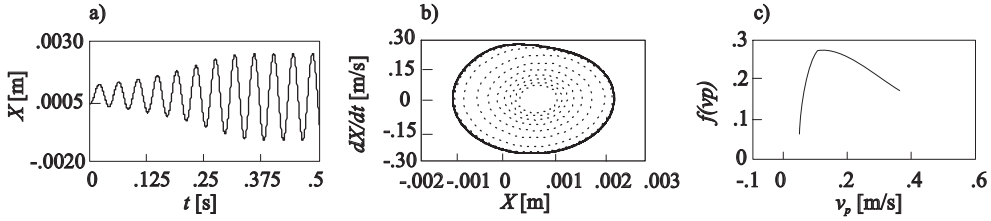

Figure 10 Vibration character at $D = 0.0$ [Ns/m]: a) displacement vs. time, b) phase plane, c) friction characteristics

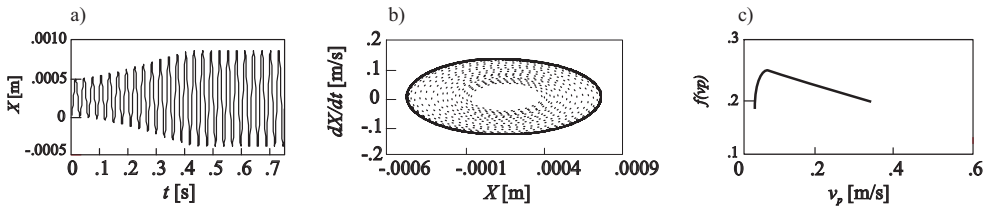

Figure 11 Vibration character at $D = 50.0$ [Ns/m]: a) displacement vs. time, b) phase plane, c) friction characteristics

As seen in Figures 10 to 13 introduction of damping diminishes amplitudes of vibration and slightly lowers their frequency from 33,6 Hz down to 33,4 Hz, and at particular value of damping coefficient – see Figure 12 the system reaches limit cycle very soon. At critical damping, Figure 13, vibration in the system disappear.

Changes of normal pressure are presented in Figures 14 to 16, with other parameters set to: $v_t = 3.0$ [m/s]; $K = 0.5 \cdot 10^6$ [N/m]; $D = 0$ [N], $\alpha = 3[°]$.

Increase of the normal pressure leads to small increase of vibration amplitude and decrease the frequency from 33.6 Hz down to 33.4 Hz.

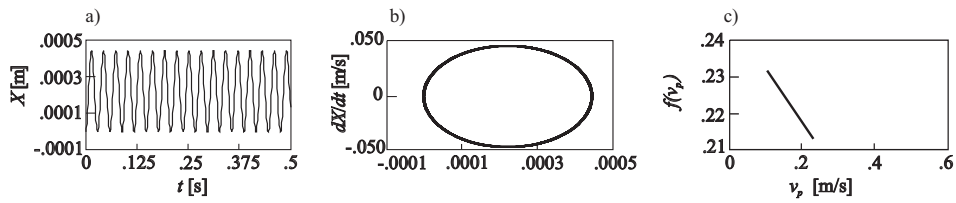

Figure 12 Vibration character at $D = 107.6$ [Ns/m]: a) displacement vs. time, b) phase plane, c) friction characteristics

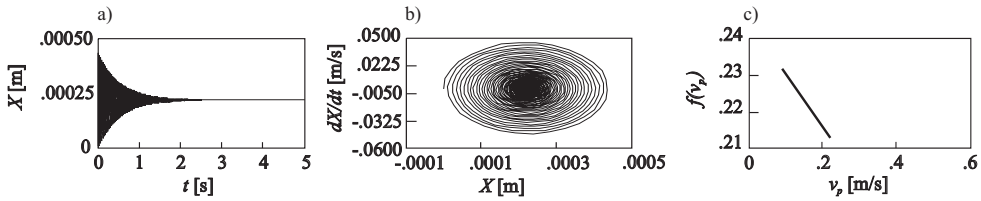

Figure 13 Vibration character at $D = 150.0$ [Ns/m]: a) displacement vs. time, b) phase plane, c) friction characteristics

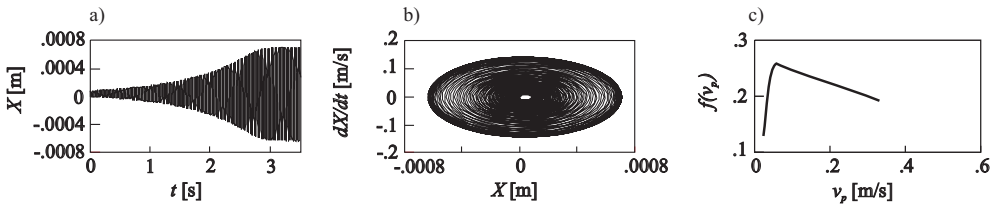

Figure 14 Vibration character at $N = 100$ [N]: a) displacement vs. time, b) phase plane, c) friction characteristics

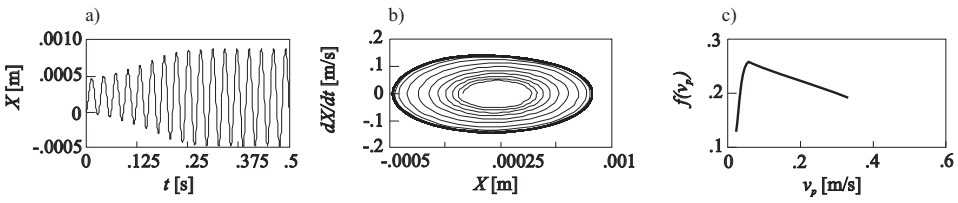

Figure 15 Vibration character at $N = 500$ [N]: a) displacement vs. time, b) phase plane, c) friction characteristics

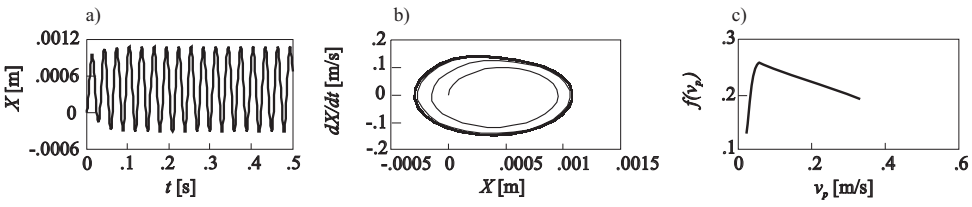

Figure 16 Vibration character at $N = 1000$ [N]: a) displacement vs. time, b) phase plane, c) friction characteristics

In the above simulation results velocity of the belt was taken constant and pressure level were independent. Later, other cases are presented when:

1. pressure level of the belt to the roller was randomly changed, with assumption of constant efficiency (output) of the conveyor system, $N\,v_t = 1500 = \text{const}$ [Nm/s], ($\alpha = 3°$; $D = 0$ [Ns/m]; $N = 1000$ N).

2. pressure level of the belt to the roller was randomly changed, with assumption of constant belt velocity, at $v_t = 3.0 = \text{const}$ [m/s].

For the first case typical views to the system behavior is shown in Figure 17, and for the second one in Figure 18.

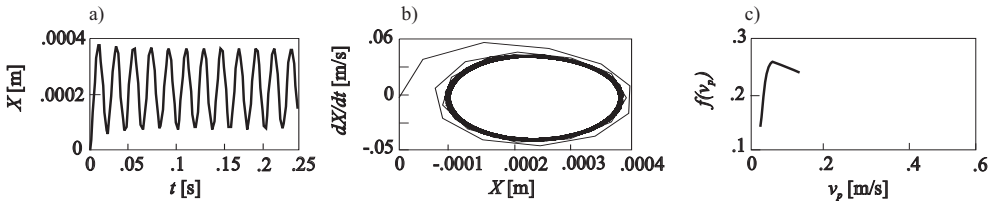

Figure 17 Vibration character at randomly changing normal pressure force N and constant output rate: a) displacement vs. time, b) phase plane, c) friction characteristics

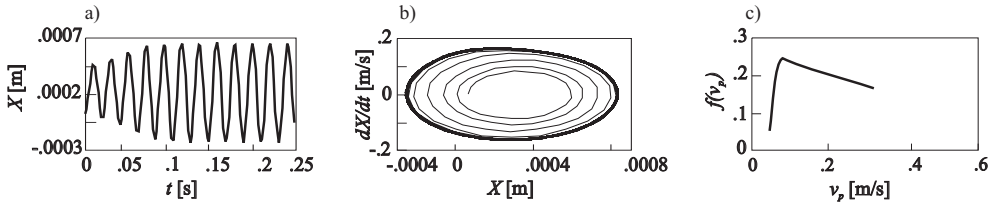

Figure 18 Vibration character at randomly changing normal pressure force N and constant belt velocity: a) displacement vs. time, b) phase plane, c) friction characteristics

Comparing vibration amplitudes in both cases one can notice at randomly changing pressure of the belt to the roller and constant efficiency resulting amplitudes are lower than in the second case. In consequence lower wear in the friction contacting elements can be expected. While character of the vibration – of the quasiharmonic type – stays the same, ranges of work in both characteristics are different.

Figure 19 and 20 shows results when pressure was lower and small damping was increased $D = 2.15$ Ns/m at $\alpha = 3°$.

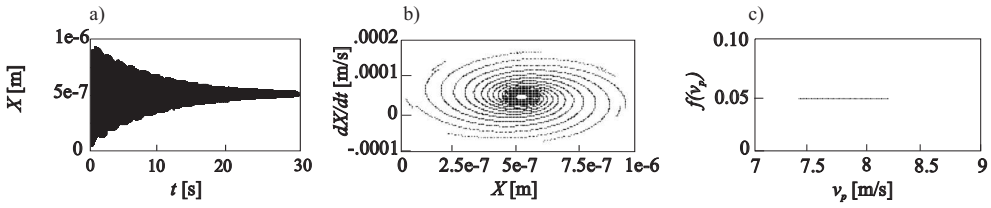

Figure 19 Vibration character at randomly changing normal pressure force $N_{av} = 10$ [N] and constant output rate at $D = 2.15$ [Ns/m]: a) displacement vs. time, b) phase plane, c) friction characteristics

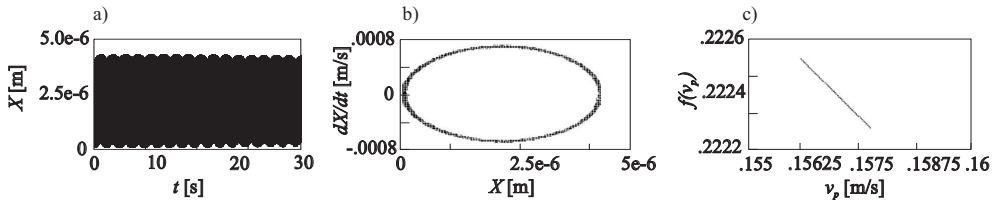

Figure 20 Vibration character at randomly changing normal pressure force $N_{av} = 10$ [N] and constant belt velocity: a) displacement vs. time, b) phase plane, c) friction characteristics

Figure 19 presents disappearing vibration at frequency of 41.5 Hz. At Figure 20 limit cycle at 47.6 Hz appears, and when damping coefficient reaches level higher than 2.15 Ns/m – vibration disappear while at lower values they increase infinitely.

When velocity and pressure are randomly changed, around value $N_{or} = 10$ N and $v = 3$ m/s, at $D = 2.15$ Ns/m, $\alpha = 3°$ limit cycle was reached at frequency of 47.5 Hz – see Figure 21.

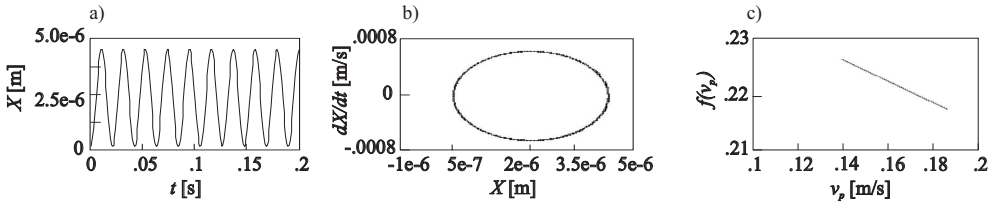

Figure 21 Vibration character at randomly changing normal pressure force $N_{av} = 10$ [N] and constant belt velocity at $D = 2.15$ [Ns/m]: a) displacement vs. time, b) phase plane, c) friction characteristics

Increase of the pressure N results in vibration shown in Figures 22 to 25.

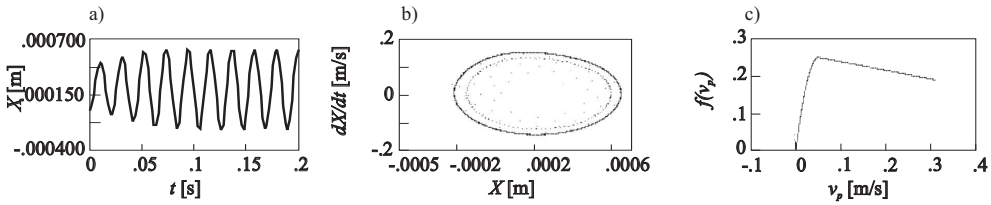

Figure 22 Vibration character at randomly changing normal pressure force $N_{av} = 1000$ [N] and constant belt velocity at $D = 2.15$ [Ns/m]: a) displacement vs. time, b) phase plane, c) friction characteristics

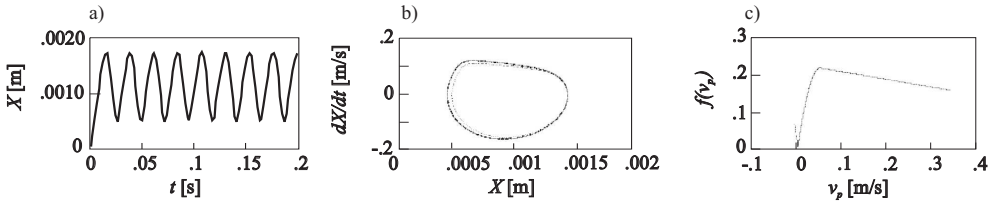

Figure 23 Vibration character at randomly changing normal pressure force $N_{av} = 5000$ [N] and constant belt velocity at $D = 2.15$ [Ns/m]: a) displacement vs. time, b) phase plane, c) friction characteristics

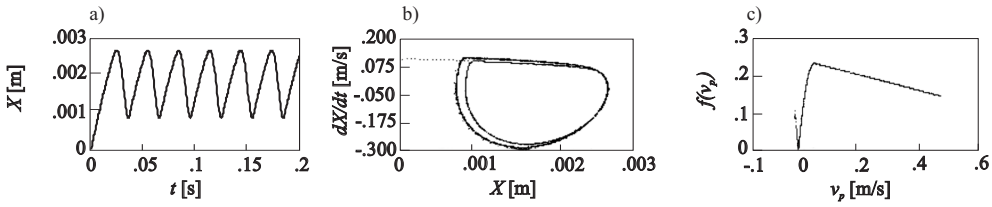

Figure 24 Vibration character at randomly changing normal pressure force $N_{av} = 10000$ [N] and constant belt velocity at $D = 2.15$ [Ns/m]: a) displacement vs. time, b) phase plane, c) friction characteristics

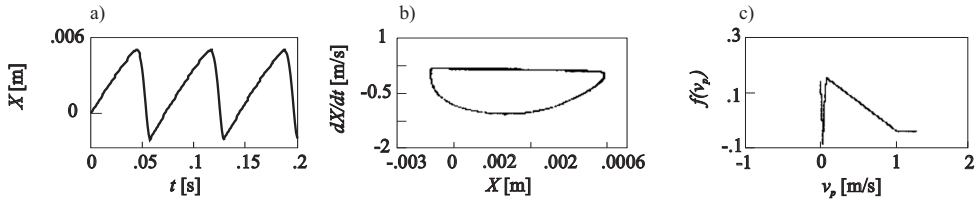

Figure 25 Vibration character at randomly changing normal pressure force $N_{av} = 20000$ [N] and constant belt velocity at $D = 2.15$ [Ns/m]: a) displacement vs. time, b) phase plane, c) friction characteristics

Results are as follows – with increasing of the pressure force amplitude of the vibration increases and, additionally, the type is changed – quasiharmonic vibration changes into stick-slip. Figures 22 to 24 show doubling of the trajectories in the phase plane, and the system works on the negative branch of the friction characteristics, see also Figure 25.

When elastic coefficient doubles its initial value, the vibration amplitude diminishes and the frequency increases from 11.4 Hz to 67.2 Hz, see Figure 26; sufficiently large damping, $D = 130$ Ns/m, causes vibration to cease – Figure 27.

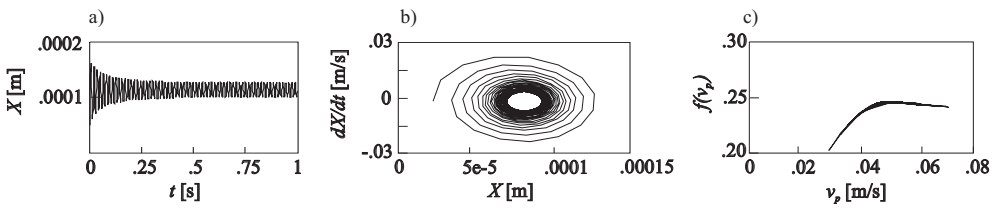

Figure 26 Vibration character at randomly changing normal pressure force $N_{or} = 500$ [N] and constant belt velocity $v_t = 3.0$ [m/s] at $D = 0$ [Ns/m], $\alpha = 1°$, $K = 2 \cdot 10^6$ [N/m]: a) displacement vs. time, b) phase plane, c) friction characteristics

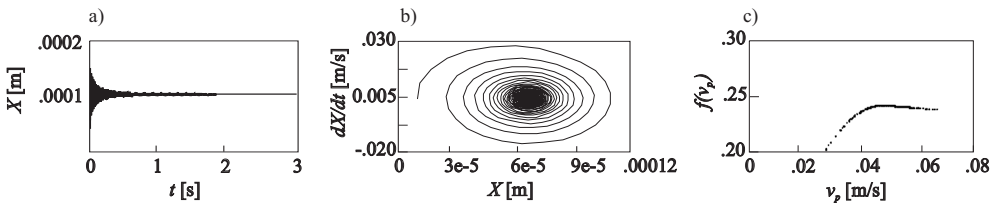

Figure 27 Vibration character at randomly changing normal pressure force $N = 500$ [N] and constant belt velocity $v_t = 3.0$ [m/s] at $D = 120$ [Ns/m], $\alpha = 1°$, $K = 2 \cdot 10^6$ [N/m]:
a) displacement vs. time, b) phase plane, c) friction characteristics

4. Conclusions

Simulation results allow to formulate the following statements:

Quantities characterizing roller vibration and the type depends on friction characteristics and the following parameter values angle of roller fixation, belt velocity, its pressure to the roller and some other system parameters.

With increase belt pressure to the roller vibration amplitude increases and the frequency decreases. Additionally, the type of vibration changes – quasiharmonic motion becomes of the stick-slip type. With increase of the stiffness amplitude of vibration decreases and the frequency increases, noise level becomes important factor of the conveyor work.

Significant limitation of appearance and level of self excited vibration in the belt-roller system is possible to occur by decreasing the angle of centering roller fixation down to the value of $\alpha < 0.9°$, and, at higher values of the angle using proper damping in the support.

Efficiency of control of the unwanted, axial self excited vibration of the roller will be easier to estimate including into the simulation model more details of the conveyor belt system.

References

[1] **Bogacz R., Ryczek B.**: *Eksperymentalno-teoretyczne badania drgań wzbudzanych tarciem suchym*, *Czasopismo Techniczne*, **10**, Politechnika Krakowska, Kraków 1996 (in Polish).

[2] **Furmanik K.**: Zagadnienie współpracy ciernej taśmy przenośnikowej z krążnikiem centrującym, *Zagadnienia Eksploatacji Maszyn*, **4**(124), 9-21, 2000 (in Polish).

[3] **Gładysiewicz L.**: Wpływ własności taśmy na opory ruchu przenośnika, *Mechanizacja i Automatyzacja Górnictwa*, **1**(341), 1999, 19-26 (in Polish).

[4] **Grimmer K. J.**: Zwei ausgewählte Probleme der Bandfördertechnik, *Fortschritt Berichte VDI Zeitschrift*, **13**(10).

[5] **Kowal J.**: *Sterowanie drganiami*, Kraków, Gutenberg, 1996, (in Polish).

[6] **Prącik M.**: Quality requirements at simulation of control of self-excited vibrations of a mechanical system, *Proceedings of 5th International Carpathian Control Conference, Zakopane Poland*, 2004.

[7] **Stefański A., Wojewoda J., Furmanik K.**: Experimental and numerical analysis of self-excited friction oscillator, *Chaos, Solitons and Fractals*, 2001, 1691-1704.

[8] **Żak S. H.**: *Systems and Control*, Oxford University Press, New York-Oxford, 2003.

[9] **Visual Solution, Inc. Westford**, *Professional VisSim & Analyze*, ver.2.0.b.